

Cardiac protection induced by urocortin-2 enables the regulation of apoptosis and fibrosis after ischemia and reperfusion involving miR-29a modulation

Isabel Mayoral-González, Eva Calderón-Sánchez, Isabel Galeano-Otero, Marta Martín-Bórnez, Encarnación Gutiérrez-Carretero, María Fernández-Velasco, Nieves Domenech, María Generosa Crespo-Leiro, Ana Maria Gómez, Antonio Ordóñez-Fernández, et al.

▶ **To cite this version:**

Isabel Mayoral-González, Eva Calderón-Sánchez, Isabel Galeano-Otero, Marta Martín-Bórnez, Encarnación Gutiérrez-Carretero, et al.. Cardiac protection induced by urocortin-2 enables the regulation of apoptosis and fibrosis after ischemia and reperfusion involving miR-29a modulation. Molecular Therapy - Nucleic Acids, 2022, 27, pp.838-853. 10.1016/j.omtn.2022.01.003 . inserm-03608891

HAL Id: inserm-03608891

https://inserm.hal.science/inserm-03608891

Submitted on 15 Mar 2022

HAL is a multi-disciplinary open access archive for the deposit and dissemination of scientific research documents, whether they are published or not. The documents may come from teaching and research institutions in France or abroad, or from public or private research centers.

L'archive ouverte pluridisciplinaire **HAL**, est destinée au dépôt et à la diffusion de documents scientifiques de niveau recherche, publiés ou non, émanant des établissements d'enseignement et de recherche français ou étrangers, des laboratoires publics ou privés.

Molecular Therapy
Nucleic Acids
Original Article

Cardiac protection induced by urocortin-2 enables the regulation of apoptosis and fibrosis after ischemia and reperfusion involving miR-29a modulation

Isabel Mayoral-González,[1,2] Eva M. Calderón-Sánchez,[2,3,10] Isabel Galeano-Otero,[2,4,10] Marta Martín-Bórnez,[1,2] Encarnación Gutiérrez-Carretero,[1,2,3] María Fernández-Velasco,[3,5] Nieves Domenech,[3,6] María Generosa Crespo-Leiro,[3,6] Ana María Gómez,[7] Antonio Ordóñez-Fernández,[1,2,3] Abdelkrim Hmadcha,[8,9] and Tarik Smani[2,3,4]

[1]Department of Surgery, University of Seville, Seville, Spain; [2]Group of Cardiovascular Pathophysiology, Institute of Biomedicine of Seville (IBiS), University Hospital of Virgen del Rocío/University of Seville/CSIC, Seville, Spain; [3]Centro de Investigación Biomédica en Red Enfermedades Cardiovaculares (CIBERCV), Madrid, Spain; [4]Department of Medical Physiology and Biophysics, University of Seville, Seville, Spain; [5]Innate Immune Response Group, IdiPAZ, La Paz University Hospital, Madrid, Spain; [6]Cardiology Department, Instituto de Investigación Biomédica de A Coruña, Complexo Hospitalario Universitario de A Coruña, Servicio Gallego de Salud, Universidade da Coruña, Coruña, Spain; [7]Signaling and Cardiovascular Pathophysiology, INSERM, Université Paris Saclay, Châtenay-Malabry, France; [8]Department of Biotechnology, University of Alicante, Alicante, Spain; [9]University of Pablo Olavide, Seville, Spain

Urocortin-2 (Ucn-2) has demonstrated cardioprotective actions against myocardial ischemia-reperfusion (I/R) injuries. Herein, we explored the protective role of Ucn-2 through microRNAs (miRNAs) post-transcriptional regulation of apoptotic and pro-fibrotic genes. We determined that the intravenous administration of Ucn-2 before heart reperfusion in a Wistar rat model of I/R recovered cardiac contractility and decreased fibrosis, lactate dehydrogenase release, and apoptosis. The infusion of Ucn-2 also inhibited the upregulation of 6 miRNAs in revascularized heart. The *in silico* analysis indicated that miR-29a and miR-451_1* are predicted to target many apoptotic and fibrotic genes. Accordingly, the transfection of neonatal rat ventricular myocytes with mimics overexpressing miR-29a, but not miR-451_1*, prevented I/R-induced expression of pro- and anti-apoptotic genes such as *Apaf-1*, *Hmox-1*, and *Cycs*, as well as pro-fibrotic genes *Col-I* and *Col-III*. We also confirmed that Hmox-1, target of miR-29a, is highly expressed at the mRNA and protein levels in adult rat heart under I/R, whereas, Ucn-2 abolished I/R-induced mRNA and protein upregulation of HMOX-1. Interestingly, a significant upregulation of *Hmox-1* was observed in the ventricle of ischemic patients with heart failure, correlating negatively with the left ventricle ejection fraction. Altogether, these data indicate that Ucn-2, through miR-29a regulation, provides long-lasting cardioprotection, involving the post-transcriptional regulation of apoptotic and fibrotic genes.

INTRODUCTION

Acute myocardial infarction (AMI) is one of the major causes of morbidity and mortality worldwide.[1] AMI sequelae, such as apoptosis of cardiac myocytes in the so-called border or risk zone near the infarct scars, are known to trigger adverse cardiac remodeling and aggravate cardiac dysfunction.[2,3] The benefits of timely and effective early revascularization after AMI are well recognized. However, the process of myocardial revascularization is associated with critical injuries that occur when oxygen-rich blood re-enters the vulnerable myocardial tissue, a phenomenon known as ischemia-reperfusion (I/R) syndrome.[4] Lethal complications of I/R injuries cause the adverse cardiac remodeling and, consequently, heart failure.[5,6] Therefore, effective strategies in cardioprotection are still eagerly needed.

In recent years, evidence demonstrated that urocortin-2 (Ucn-2) has cardioprotective effects on myocardial I/R injuries and heart failure.[7] Ucn-2 is an endogenous peptide belonging to the corticotropin-releasing factor (CRF) family. Ucn-2 binds with high affinity to the receptor CRF-R2 that is highly expressed in the cardiovascular system.[8] The administration of Ucn-2 evokes important changes in the cardiovascular system, such as human coronary vasodilatation,[9] and triggers potent cardioprotective effects against I/R injuries since it decreases the infarct size and prevents harmful cell death.[10] Similarly, the other isoform Ucn-1 induces positive inotropic and lusitropic effects in rats,[11] improves the intracellular calcium concentration ($[Ca^{2+}]_i$) handling in I/R,[12] and efficiently

Received 11 May 2021; accepted 7 January 2022;
https://doi.org/10.1016/j.omtn.2022.01.003.

[10]These authors contributed equally

Correspondence: Tarik Smani, Instituto de Biomedicina de Sevilla (IBiS), Hospital Universitario Virgen del Rocío, Avenida Manuel Siurot S/N, Sevilla 41013, Spain.
E-mail: tasmani@us.es
Correspondence: Abdelkrim Hmadcha, University of Pablo Olavide, Sevilla 41013, Spain.
E-mail: khmadcha@upo.es

This is an open access article under the CC BY-NC-ND license (http://creativecommons.org/licenses/by-nc-nd/4.0/).

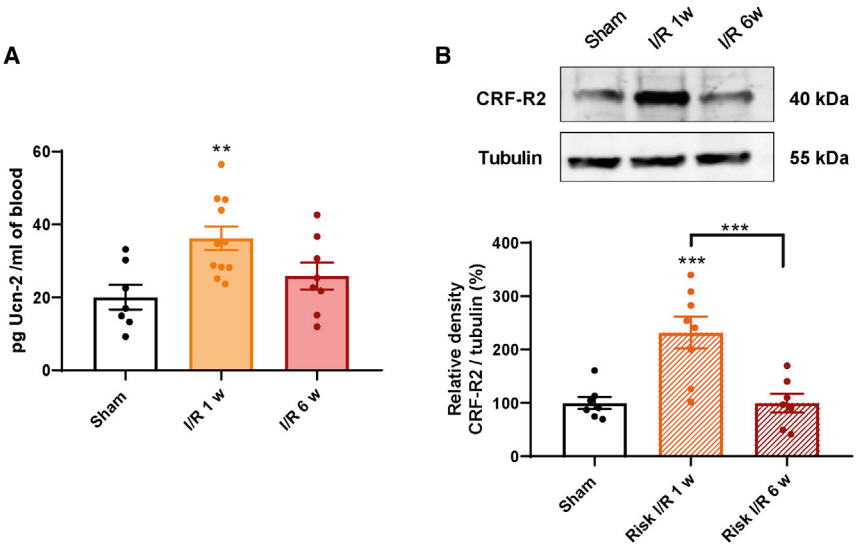


Figure 1. I/R increases of circulating Ucn-2 levels and the expression of CRF-R2

(A) Bar graph shows the concentration of circulating Ucn-2 in serum of rats from sham, I/R 1 week (I/R 1w) and 6 weeks (I/R 6w) after surgery (n = 7–11). (B) Plot of western blot and bar graph summarizing the expression of CRF-R2 expression and tubulin in rats' heart from sham, I/R (1 and 6 weeks) after surgery (n = 8). Values are means ± standard error of the mean. $^{**}p < 0.01$; *** $p < 0.001$.

protects hearts from I/R injuries by the modulation of apoptotic genes, such as *Cd40lg*, *Xiap*, and *Bad*.[13] The infusion of Ucn-2 into the rat I/R model also promotes cardioprotection, involving changes in the expression of microRNAs (miRNAs), which play major role in the post-transcriptional regulation of genes.[14] miRNAs are small non-coding RNAs that regulate a plethora of cellular processes related to AMI, including cardiac myocyte apoptosis, necrosis, and fibrosis.[15] They play critical roles in heart function under pathophysiological conditions and also in different cardioprotection strategies.[16,17] Recently, we demonstrated that the levels of different miRNAs changed rapidly into the bloodstream of patients suffering from AMI with ST-segment elevation (STEMI) undergoing primary percutaneous coronary intervention (pPCI), and were related to the development of the adverse cardiac remodeling.[18]

In the present study, we evaluated the role of Ucn-2 in the regulation of miRNAs expression under I/R, focusing on a list of circulating miRNAs whose levels changed in infarcted patients after pPCI. We further examined the role of miRNAs in the regulation of pro-fibrotic and apoptotic genes induced by I/R.

RESULTS

I/R increases circulating Ucn-2 and the expression of CRF-R2 in heart tissue

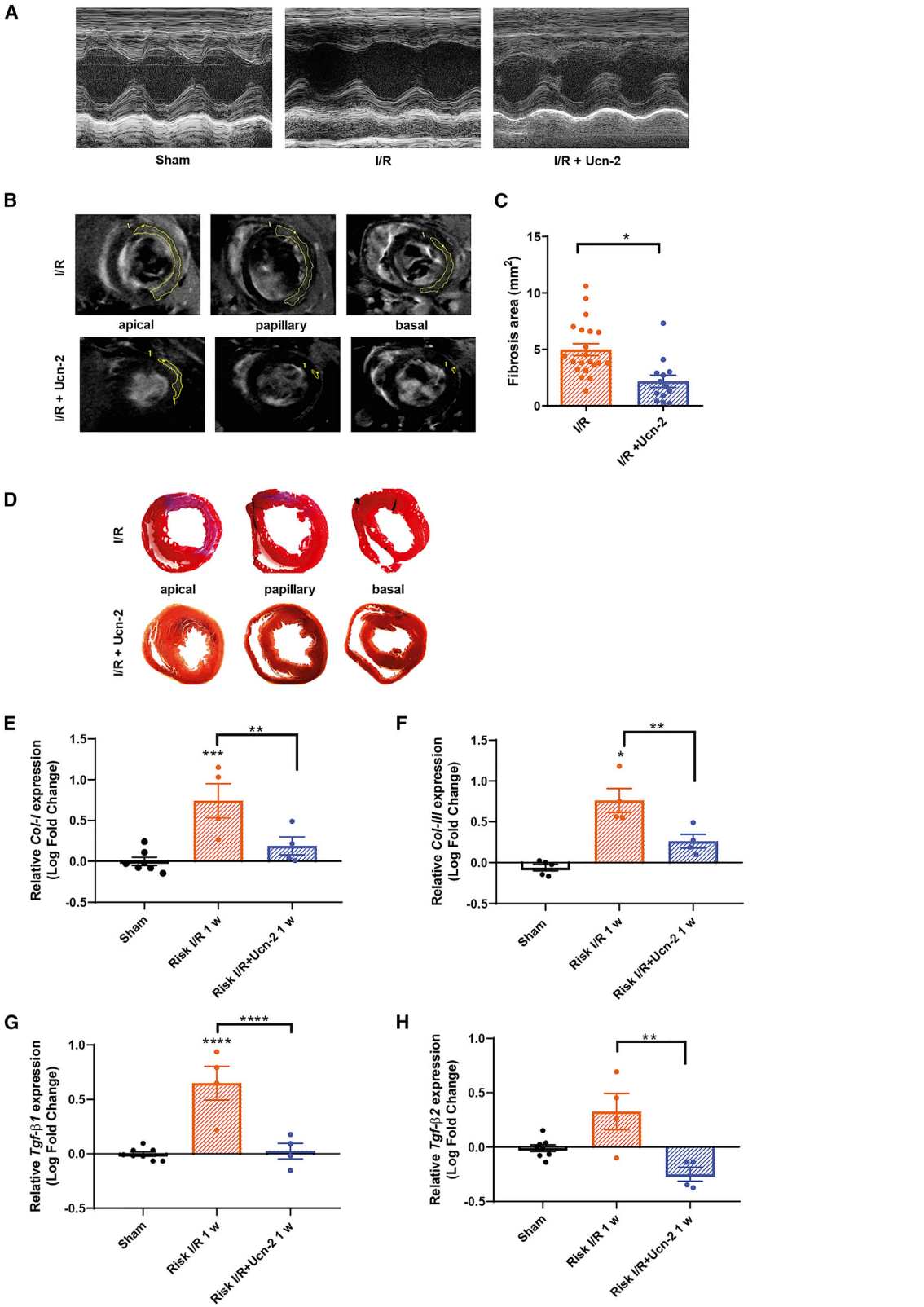
Since Ucn-2 is an endogenous stress-related peptide, we examined its concentration in serum of I/R rat model following the experimental protocol illustrated in Figure S1A. Figure 1A shows that the concentration of Ucn-2 increased significantly 1 week after heart's intervention, as compared with sham; meanwhile, it decreased 6 weeks after surgery. We also assessed the expression of Ucn-2 receptor (CRF-R2) in risk zone of the infarcted heart. Figure 1B shows that the expression of CRF-R2 was significantly increased 1 week after I/R, comparing to sham. In contrast, the expression of CRF-R2 was restored 6 weeks after surgery. Therefore, the level of circulating Ucn-2 and the expression of CRF-R2 increased transiently after the heart infarction and its revascularization.

Ucn-2 recovers heart contractility and prevents I/R-induced fibrosis

We investigated the cardioprotective effect of Ucn-2 (150 μg/Kg) infused 5 min before reperfusion, using different approaches. Data in Figure 2A and Table 1 indicate that 1 week after surgery the left ventricle ejection fraction (LVEF) and the left ventricle fractional shortening (LVFS), as well as the left ventricular end-diastolic volume (LVEdV) and the left ventricular end-systolic volume (LVEsV), recovered significantly in Ucn-2-treated rats as compared with I/R non-treated rats. Meanwhile, the I/R-induced increase in the left ventricle diastolic diameter was not affected by Ucn-2. Next, we examined the effect of Ucn-2 on cardiac fibrosis. As shown in Figures 2B–2D, the administration of Ucn-2 decreased the fibrotic areas of the infarcted hearts assessed *in vivo* by cardiac magnetic resonance and by Masson's trichrome staining. Moreover, Figures 2E–2H shows that the expression of pro-fibrotic genes *Collagen*-I (*Col*-I), *Collagen*-III (*Col*-III), *Transforming Growth Factor β-1* (*Tgf-β1*), and *Transforming Growth Factor β-2* (*Tgf-β2*) increased significantly in the risk zone of hearts isolated 1 week after I/R. By contrast, rats treated with Ucn-2 showed significantly reduced expression of these pro-fibrotic genes.

Ucn-2 prevents I/R-induced apoptosis

To further evaluate the cardioprotection exerted by Ucn-2, we examined its action on cardiac myocyte viability and death. As illustrated in Figure 3A, the administration of Ucn-2 decreased significantly I/R-evoked lactate dehydrogenase (LDH) concentrations, increased 24 h after I/R. Following the experiment protocol outlined in Figures S1A and 3B shows that Ucn-2 infusion in I/R rat markedly decreased the number of apoptotic cardiac myocytes, as assessed by TUNEL assay. Ucn-2 treatment also tended to decrease I/R-evoked caspase 3 cleavage (Figure 3C). To confirm these results, we examined Ucn-2 effect on adult rat ventricle myocytes (ARVM), using annexin V staining. As depicted in Figures 3D–3F, Ucn-2 pre-treatment of cardiac myocytes exposed to I/R decreased the number of apoptotic cells stained by annexin V, while it preserved the number of living cells. Altogether, these data indicate that the infusion of Ucn-2 at the onset of reperfusion preserves cardiac cell viability and attenuates apoptosis.



(legend on next page)

Ucn-2 modulates the expression of miRNAs in the heart under I/R

Given the importance of the post-transcriptional regulation of the expression of genes in cardiac pathophysiological processes,[14,19] we examined whether Ucn-2 could regulate the expression of miRNAs in hearts excised from I/R rats model. We selected a list of miRNAs based on the analysis of circulating miRNAs released in patients with STEMI who underwent revascularization with pPCI, as described recently,[18] since little is known about the role of those miRNAs in I/R and whether they can be a good target for cardioprotective drugs. Figure 4A shows a list of circulating miRNAs released in the serum of STEMI patients 3 h after the angioplasty. The expression of miR-29a, miR-103, miR-125a-3p, miR-133, miR-139-3p, miR-320, miR-324-3p, miR-324-5p, miR-339-5p, miR-423_1, miR-451_1*, and miR-499-5p were also detected in heart samples isolated from atrium biopsies of ischemic patients with heart failure (HF) (Figure 4B). Based on these findings, we examined the expression of these 12 human miRNAs in I/R rat ventricle isolated from the risk area. As illustrated in Figures 4C–4H, the expression of miR-29a, miR-103, miR-133, miR-339-5p, miR-423_1, and miR-451_1* was significantly upregulated at 24 h and 1 week after I/R, except for miR-133, which showed a downregulation at 1 week after I/R. In contrast, the administration of Ucn-2 at 5 min before heart revascularization prevented significantly the I/R-induced upregulation of these miRNAs, excluding miR-423_1, which was not sensitive to Ucn-2 at 24 h after I/R. Figure S2 shows that I/R evoked a significant increase in the expression of miR-125a, miR-139, miR-320, and miR-324-3p at 24 h, but not of miR-324-5p or miR-499_1, while the administration of Ucn-2 did not prevent the overexpression of these miRNAs. Therefore, Ucn-2 efficiently modulated the expression of some miRNAs associated with pPCI in STEMI patients, which are altered by I/R in heart tissue of rats.

miR-29a and miR-451_1* are predicted to modulate the expression of genes related to apoptosis and the cell survival pathway

To determine target genes of miR-29a, miR-103, miR-133, miR-339-5p, miR-423_1, and miR-451_1*, we performed an *in silico* analysis using PANTHER software. As illustrated in Figure 5A, the analysis generated a pie chart suggesting that miRNAs have predicted target genes that are involved in the pathways of apoptosis and fibrosis. Specifically, 41 signaling pathways are mainly implicated in cellular processes associated with post-AMI, such as apoptosis and fibrosis. Interestingly, we found that only miR-29a and miR-451_1* are predicted to target 16 and 17 apoptotic genes, and 14 and 18 genes related to fibrosis, respectively (Figure 5B).

Based on this analysis and to assess the role of miR-29a and miR-451_1* in the regulation of those predicted genes, we performed the quantitative real-time PrimePCR array, using the Bio-Rad (Hercules, CA) predesigned assay specifically for apoptosis and survival pathway (Figure S3A). Experiments were performed in neonatal rat ventricular myocytes (NRVM) transfected with mimics of miRNAs to overexpress miR-29a and miR-451_1*, under an *in vitro* I/R protocol as explained in Figure S1B. First, we checked whether the expression of miR-29a and miR-451_1* are similarly sensitive to I/R in NRVM and adult heart. Accordantly, Figures S3B and S3C confirm that I/R enhanced the expression of miR-29a and miR-451_1*, while Ucn-2 significantly inhibited both miRNAs in a similar way in NRVM and in adult rat heart. Second, Figures S3D and 3E show that NRVM transfection with mimics of miR-29a and miR-451_1* successfully increased the levels of miR-29a and miR-451-1*.

Figure 5C and Table S1 show that 56 genes were upregulated and 20 downregulated 24 h after I/R in NRVM. By contrast, in NRVM transfected with mimics of miR-29a and miR-451_1*, 56 and 49 genes were downregulated, while 20 and 27 genes were upregulated, respectively (Figures 5D and 5E; Table S1). These data indicate that mimics of miR-29a and miR-451_1* reverted the expression of many apoptotic genes overexpressed under I/R.

miR-29a regulates the expression of I/R-induced apoptotic and fibrotic genes

To verify the results of the PrimePCR array, we examined the expression of six selected genes in NRVM transfected with mimics of miR-29a and miR-451_1* under I/R. The selection of these genes was based on their fold change rates as well as their implication in I/R-related processes, as published elsewhere.[20–22] Namely, we investigated the expression of *Apoptosis Inducing Factor mitochondria associated 1* (*Aifm1*), *Apoptosis Protease-Activating Factor-1* (*Apaf1*), *B-Cell Lymphoma 2* (*Bcl-2*), *Cytochrome c* (*Cycs*), *Heme Oxygenase 1* (*Hmox-1*), and *Mitogen-Activated Protein Kinase 8* (*Mapk-8*). Figures 6A and 6B show that the expression of *Apaf-1* and *Hmox-1* increased significantly in I/R, as compared with controls. Figure 6C indicates that the expression of *Cycs* slightly increased under I/R, although not significantly. However, the expression of *Aifm-1*, *Bcl-2*, and *Mapk-8* was not affected by I/R, as compared with controls (Figures 6D–6F). Conversely, mimic of miR-29a, but not of miR-451_1*, prevented I/R effects on *Apaf-1*, *Hmox-1*, and *Cycs* (Figures 6A–6C). Meanwhile, miR-29a enhanced the expression of *Aifm-1* (Figure 6D) and decreased the expression of *Mapk-8* (Figure 6F) under I/R. In contrast, miR-451_1* mimic significantly increased the expression of *Hmox-1* and *Mapk-8*, comparing to their

Figure 2. Ucn-2 improves contractility and prevents I/R-induced fibrosis

(A) Representative M-mode echocardiographic images evaluated 1 week after the intervention in sham, I/R rats, and in rats infused with 150 μg/kg Ucn-2 (I/R + Ucn2). (B) Representative *in vivo* cardiac magnetic resonance images taken from I/R and I/R + Ucn-2 rats. Gadolinium was used as contrast. The fibrotic area is delimited by yellow lines. (C) Bar graph showing summary data of fibrotic areas in I/R and I/R + Ucn-2 rats. (D) Representative Masson's trichrome staining of transverse heart sections from I/R and I/R + Ucn-2. Healthy tissue is stained by red, while fibrotic tissue in the infarcted zone is stained in blue. (E–H) Bar graphs show the effect of Ucn-2 on the expression of profibrotic genes, collagen I (*Col-I*, E), collagen III (*Col-III*, F), transforming growth factor *β1* (*Tgf-β1*, G), and *Tgf-β2* (H), examined in the risk zone of the infarcted hearts 1 week after surgeries. Samples were from Sham, I/R, and I/R + Ucn-2 groups. Gene's relative expression was calculated using the $2^{-\Delta\Delta Ct}$ method after normalization to the internal control β-actin. Data are relative expression of Log fold change of means ± standard error of the mean (n = 4–8). *p < 0.05; **p < 0.01; ***p < 0.001; ****p < 0.0001.

Table 1. Data summary (mean ± standard error of the mean) of hemodynamic parameters evaluated in rats 1 week after surgery in the following experimental group: Sham, I/R, and I/R + Ucn-2

	LVEdV (mL)	LVEsV (mL)	LVdD (mm)	LVEF (%)	LVFS (%)
Sham (n = 10)	0.42 ± 0.02	0.12 ± 0.01	5.91 ± 0.18	71.84 ± 1.23	19.98 ± 1.90
I/R (n = 12)	0.50 ± 0.03[a]	0.20 ± 0.02[a]	6.85 ± 0.27[a]	60.16 ± 2.04[a]	16.77 ± 1.1[a]
I/R + Ucn-2 (n = 15)	0.40 ± 0.02b	0.13 ± 0.01[b]	6.46 ± 0.16	66.43 ± 0.68[a,b]	18.16 ± 3.20

LVdD, left ventricle diastolic diameter; LVEdV, left ventricle end-diastolic volume; LVEsV, left ventricle end-systolic volume.
[a]$p < 0.05$ in Sham vs I/R
[b]$p < 0.05$ in I/R vs IR + Ucn2.

levels in I/R (Figures 6C and 6F). The expression of *Bcl-2* was not affected either by I/R or miRNAs mimics. Moreover, we analyzed whether miR-29a and miR-451_1* could target pro-fibrotic genes in NRVM, as is the case of the effect of Ucn-2 in the tissue of adult heart shown previously in Figure 2. Figures 6G and 6H shows that I/R induced a small but significant upregulation of *Col-I* and *Col-III*, which was significantly downregulated by miR-29a. Of note, miR-451_1* also failed to modulate the expression of *Col-I* and *Col-III*. These data indicate that miR-29a, but not miR-451-1*, modulated the I/R-induced overexpression of *Apaf-1*, *Hmox-1*, *Cycs*, *Col-I*, and *Col-III*.

Signaling pathway involved in miR-29a regulation by Ucn-2

Once we determined that miR-29a efficiently modulated I/R-induced changes in the expression of apoptotic and fibrotic genes, we studied the signaling pathway involved in the regulation of miR-29a by Ucn-2 applied in NRVM under I/R (Figure S1C). Figure 6I shows that NRVM treatment with Ucn-2 (10 nM) before reperfusion inhibited I/R-induced miR-29a overexpression, whereas NRVM pretreatment with astressin (0.5 μM), the specific antagonist of the CRF-R2 receptor,[23] significantly attenuated the Ucn-2 effect. CRF-R2 is known to couple Gs/cAMP/protein kinas A (PKA) signaling; therefore, we investigated whether Ucn-2 action was mediated by PKA or Epac (exchange protein directly activated by cAMP). Our data show that NRVM pretreatment with ESI-05 (10 μM), a specific inhibitor of Epac2,[24] abolished Ucn-2 downregulation of miR-29a. By contrast, PKA inhibition with H89 (1 μM) did not significantly affect Ucn-2 downregulation of miR-29a. Finally, because Epac activates the Ras1-ERK1/2 pathway,[25] we examined whether ERK1/2 participates in Ucn-2 action. Nevertheless, the inhibition of ERK1/2 by PD 098059 (5 μM)[26] did not inhibit significantly the Ucn-2 effect on miR-29a under I/R. Altogether, these data demonstrate that the administration of Ucn-2 before reperfusion modulated the expression miR-29a through the activation of CRF-R2 and Epac2.

I/R-induced changes in the expression of apoptotic genes in rat ventricle

To confirm whether these genes are relevant in the adult infarcted heart, we examined their expression in I/R rats infused with Ucn-2. Figures 7A–7C show that mRNA expression of *Hmox-1*, *Aifm-1*, and *Apaf-1* were increased in risk zones 24 h after I/R, but it significantly decreased 1 week after the intervention. Moreover, the administration of Ucn-2-blocked I/R-evoked *Hmox-1* upregulation, while it enhanced I/R-induced expression of *Aifm-1*. In contrast, Figure 7D shows that mRNA expression of *Cycs* significantly decreased 24 h, but it recovered after 1 week after I/R. The expression of *Cycs* as well as *Apaf-1* was not affected by Ucn-2 (Figures 7C and 7D). At the same time, we did not observe significant changes in the expression of *Mapk-8* under any experimental conditions, while Ucn-2 induced a *Bcl-2* increase at 24 h after I/R (Figure S4). Interestingly, as shown in Figures 7E and 7F, the protein expression of HMOX-1 and AIFM-1 was significantly increased in risk zone of I/R rats 24 h after surgery, but Ucn-2 potently reduced HMOX-1 expression and tended to decrease the upregulation of AIFM-1. By contrast, CYCS protein was not affected by I/R nor by Ucn-2 (Figure 7G).

Finally, we assessed the expression of these genes in ventricle biopsies of patients with HF of ischemic origin. Figure 8A shows that only the expression of *Hmox-1* was significantly increased, as compared with a healthy ventricle sample. The expression of *Apaf-1* and *Aifm-1* slightly, but not significantly, trend to increase in those patients. Meanwhile, the expression of *Mapk-8* and *Cycs* tended to decrease in these samples. Interestingly, the analysis of a possible correlation between patients' LVEF and these genes expression shows significant negative correlations between the expression of *Hmox-1*, *Mapk-8*, and *Cycs*, with the LVEF of the patients, whereas the expression of *Apaf-1* and *Aifm-1* did not correlate with the LVEF (Figures 8B–8F). Altogether, these results suggest that patients with HF F HFmight overexpress genes related to apoptosis in a function of the severity of their HF, although a greater number of samples is necessary to confirm this preliminary observation.

DISCUSSION

Despite the overwhelming advances in cardiovascular therapies, HF after an AMI remains the leading cause of mortality and morbidity in humans. Therefore, strategies of cardioprotection are of major interest to limit I/R injuries and cardiac myocyte loss after AMI.[27] This study confirms the important protective role of the administration of Ucn-2 at early reperfusion, which mitigates I/R injuries. We observed a significant and transient increase in circulating Ucn-2 and the expression of its receptor CRF-R2, 1 week after I/R. This result agrees with previous studies, which proposed Ucn-2 as a potential diagnostic and prognostic biomarker for cardiovascular diseases.[28,29] Ucn-2 belongs to the stress hormone CRF family; therefore, our data confirm that, under the stress caused by I/R, the heart enhances not only the circulating Ucn-2, but also its CRF-R2 receptor to activate the related signaling pathway in the injured heart. Moreover, we demonstrate that the intravenous infusion of Ucn-2 improves cardiac contractility after I/R, since it increases the LVEsV and decreases the LVEdV, indicating successful heart contraction and relaxation. In addition, using different approaches we demonstrate that Ucn-2 decreases significantly I/R-induced fibrosis, which

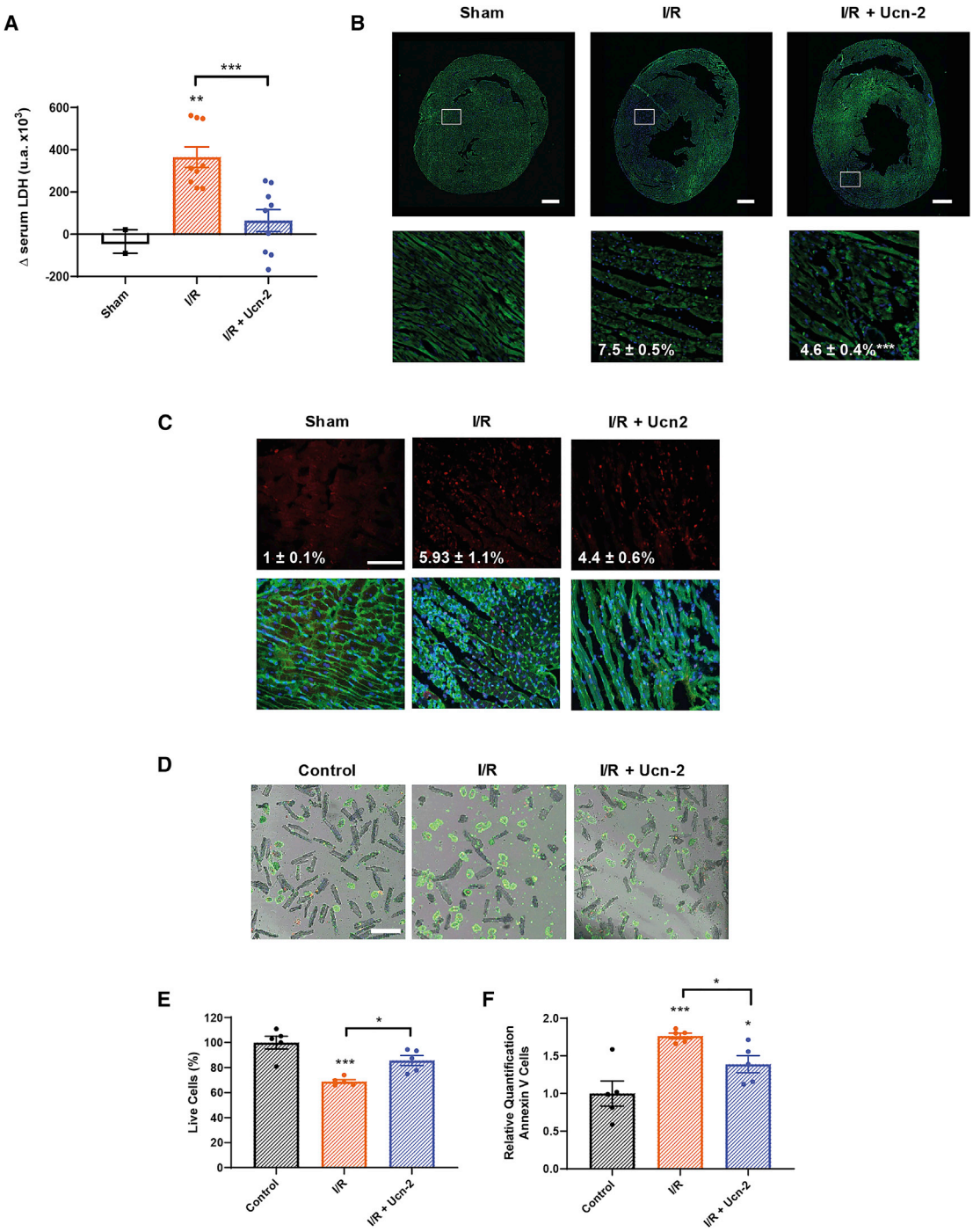


Figure 3. Ucn-2 attenuates the release of LDH and apoptosis

(A) Bar graph shows the level of LDH in the serum of rats from Sham, I/R and I/R + Ucn-2, 24 h after surgery. (B) Representative snapshot of TUNEL staining (green) in adult heart section from rats of the three experimental groups. Top: images taken with a 10× objective, scale bar = 1 mm. Bottom: images cropped from upper ones. (C) Representative images of heart sections stained for detection of cleaved caspase 3 (upper panel) captured with a 40× objective. Scale bar, 100 μm. Lower panel shows merge images of heart's section stained with caspase 3 in red, wheat germ agglutinin (WGA) in green and DAPI in blue used for nuclear staining. (D) Representative images of annexin V (green) staining in adult cardiac myocytes cells. Images are from untreated cells (control), and from cells exposed to I/R (30 min/24 h each) ± Ucn-2 (30 nM). Image were taken with a 20× objective. Scale bar, 100 μm. (E and F) Summary data showing the percentage of unstained live cardiac myocytes, and annexin V-labeled cells related to control. Values are means ± standard error of the mean (n = 4–6). *$p < 0.05$; **$p < 0.01$; ***$p < 0.001$

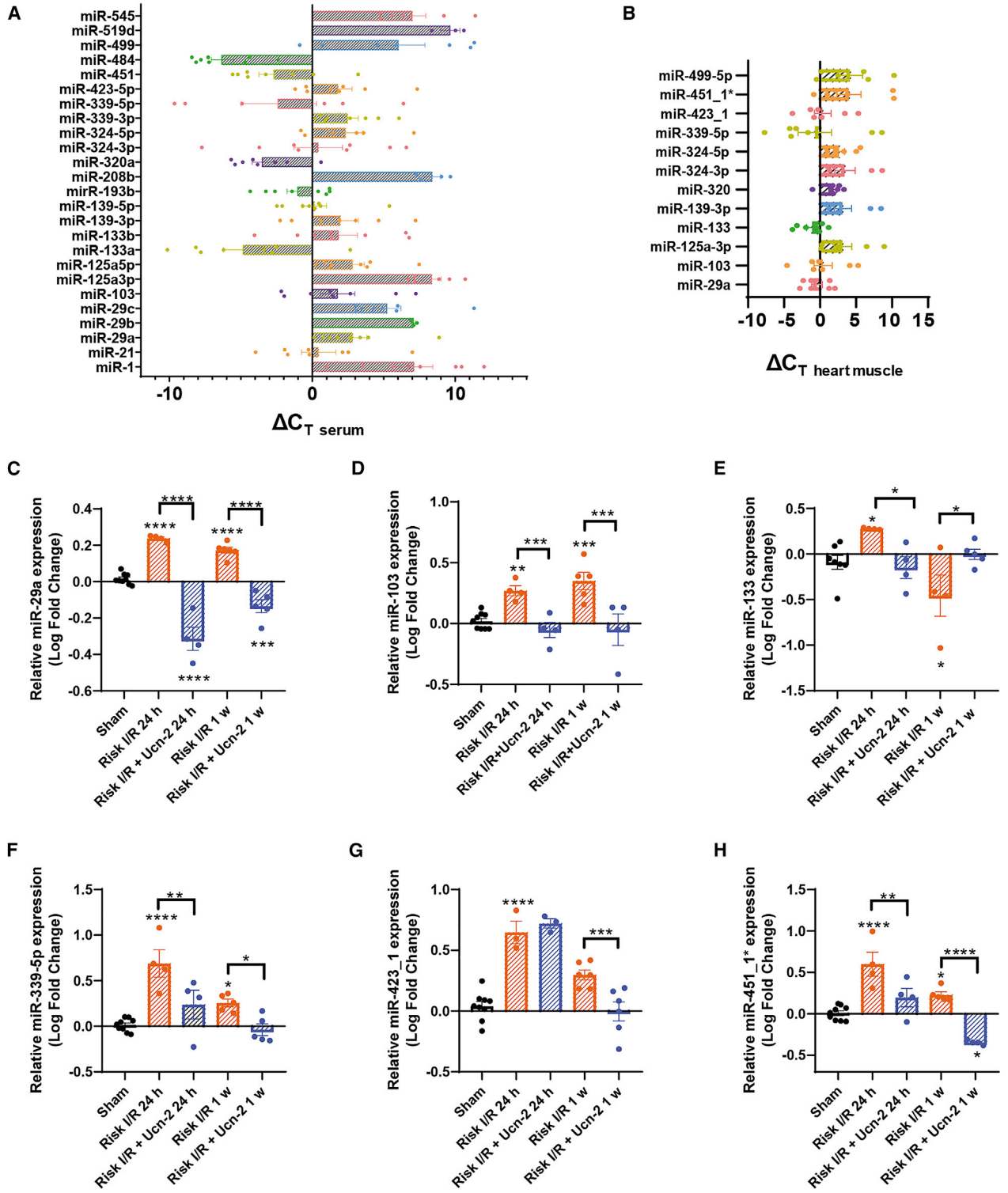


Figure 4. miRNAs expression in serum and heart tissue of STEMI patients, and in rat cardiac ventricle risk zone

(A) Bar graph summarizing microarray results indicating release of circulating miRNAs examined in the serum of STEMI patients 3–6 h after pPCI. (B) Bar graph shows the detection of selected miRNAs in the atrium of ischemic patients with HF. ΔCt represents the level of Ct of miRNAs compared to the endogenous control. Values are means ±

(legend continued on next page)

preserves myocardial compliance and prevents impaired cardiac diastolic and systolic function evoked by I/R.

I/R-induced cardiac cell death in affected hearts is another important factor contributing to cardiac dysfunction and cardiac remodeling. Here, we demonstrate that Ucn-2 reduces the LDH amount, and we observe less cleaved caspase 3 staining and DNA fragmentation, indicative of apoptosis, in Ucn-2-infused I/R rats. Annexin V staining further confirms that Ucn-2 prevents ARVM death and increases cell survival, in accordance with our previously published data.[10,14]

One of the limitations of the infusion of cardioprotective drugs is related to their limited benefits duration owing to their short half-life. Recent studies indicated that Ucn-2 gene transfer provides a sustained increase in the concentration of plasma Ucn-2 and enhanced cardiac function in normal mice and in mice with HF,[30,31] although its role in modulating I/R stress was not assessed. Herein, we provide evidences demonstrating that Ucn-2 modulates changes in miRNAs, post-transcriptional gene expression, and protein expression, in agreement with previous studies.[14,32] We decided to study the effect of Ucn-2 on miRNAs that have been recently detected in blood samples of STEMI patients undergoing pPCI[18] and in failing heart samples, because little is known about the role of those human miRNAs in cardiac function after I/R. Our results using adult rats and isolated cardiac myocytes unveil the ability of Ucn-2 to modulate the expression of six of those miRNAs that are rapidly released to the blood stream after pPCI in STEMI patients. In fact, we demonstrate that Ucn-2 infusion prevents the I/R-evoked upregulation of miR-29a, miR-103, miR-133, miR-339-5p, miR-423_1, and miR-451_1 in rats. This effect was even sustained 1 week after heart reperfusion, indicating at least a medium lasting action of Ucn-2 on miRNA dysregulation.

Based on the *in silico* and PrimePCR findings, we found that miR-29a and miR-451_1* possibly target many genes associated with apoptosis and fibrosis, two prevalent pathways during early adverse cardiac remodeling. We demonstrate that the overexpression of miR-29a, but not miR-451_1*, efficiently prevents the expression of collagen mRNA, indicating fibrosis inhibition in agreement with recent studies that showed that miR-29a inhibits fibrosis in myocardial infarcted rats,[33] in heart stressed with isoproterenol by downregulating the expression of *DNA Methyltransferase enzymes A* (*Dnmt3a*),[34] and in heart derived from chemotherapy.[35] Furthermore, miR-29a overexpression prevents I/R-induced upregulation of *Apaf-1*, *Cycs*, and *Hmox-1*; meanwhile, it increases the expression of *Aifm-1*. As known, the intrinsic mitochondrial apoptotic pathway is initiated after reperfusion by the release of *Cycs* into the cytoplasm, which stimulates *Apaf-1* and procaspase-9 in the apoptosome, inducing apoptosis.[36–38] Thus, *Apaf-1*, *Aifm-1*, and *Cycs* are considered pro-apoptotic genes.

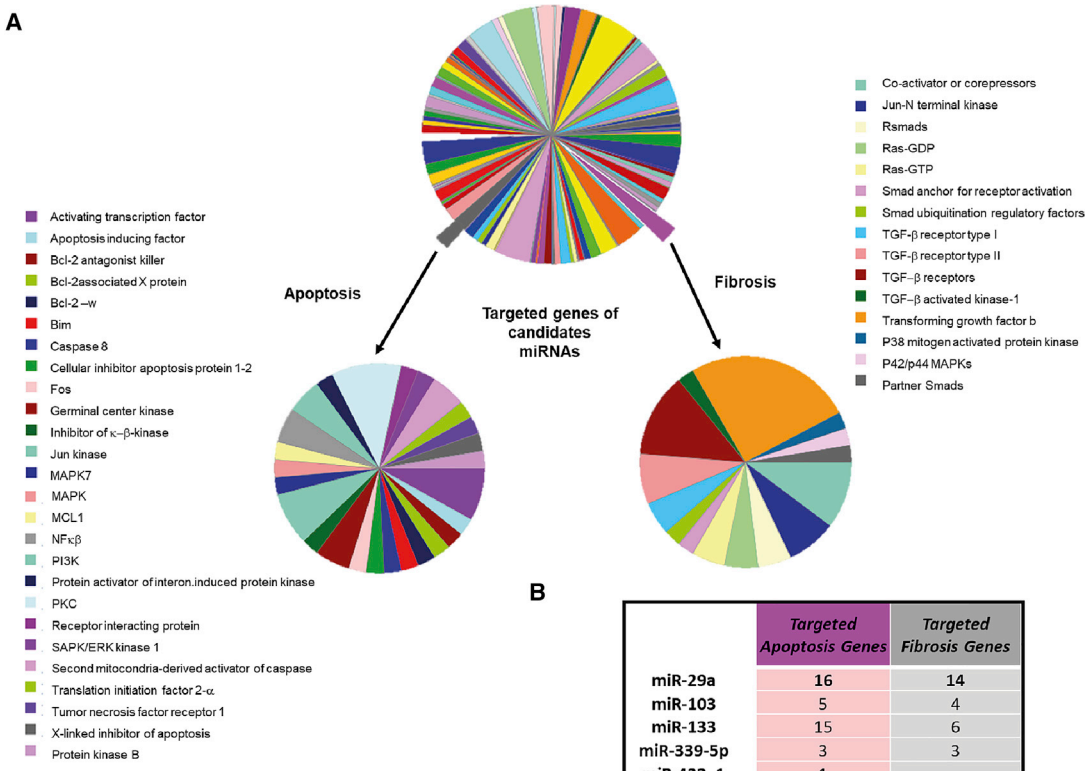
By contrast, *Hmox-1* is considered anti-apoptotic and cardioprotective. For instance, its gene delivery prevents cardiac remodeling and preserves cardiac function after myocardial infarction, as described previously.[39] Other studies demonstrated that the transplantation of mesenchymal stem cells overexpressing *Hmox-1* conferred cardioprotection against ischemic injury in heart and skeletal muscle.[40,41] There is a general consensus that cardiac myocyte activates both pro- and anti-apoptotic pathways during the progressive transition of the heart from a situation of adaptation to one of maladjustment after I/R.[42] Therefore, miR-29a and its predicted target genes could be potential regulators of a balance between pro- and anti-apoptotic processes. miR-29a has been reported to play other beneficial roles in cardiovascular homeostasis, such as cardiac hypertrophy[43] and modulation of cardiac cell metabolism,[44] indicating their potential features as therapeutic agents.

In this study, we also show in adult rat heart that HMOX-1 can be regulated by Ucn-2, in the same way as miR-29a, both at mRNA and protein levels. By contrast, Ucn-2 modulates differentially AIFM-1 at the mRNA and protein levels, indicating that perhaps Ucn-2 affects the post-translational process of some proteins. This finding suggests that the protective effect of Ucn-2 does not occur exclusively through miR-29a and may involve other mediators that could act differentially in post-transcriptional and post-translational processes. Interestingly, we demonstrate that Ucn-2 regulates the expression of miR-29a through the activation of CRF-R2 and Epac2, which is consistent with the role of Epac2 on miR-139-3p and miR-324 modulation by Ucn-1 isoform in cardiac myocytes.[14]

Furthermore, we provide preliminary data showing that ischemic patients with HF overexpress *Hmox-1*, while the expression of other apoptotic genes seem not significantly altered. We demonstrate a negative correlation between the LVEF of patients with HF and the expression of *Hmox-1*, *Cycs*, and *Mapk-8*, which may be related to the *Cycs*-mediated cell death pathway. However, the overexpression of *Hmox-1* was unexpected since this gene is thought to exert anti-inflammatory and anti-apoptotic effects post-AMI.[45] Perhaps, the overexpression of *Hmox-1* may play a role in sustaining and protecting the still non-affected tissue of the infarcted heart in patients with HF when their LVEF is severely compromised. Further experiments are needed to clarify these data.

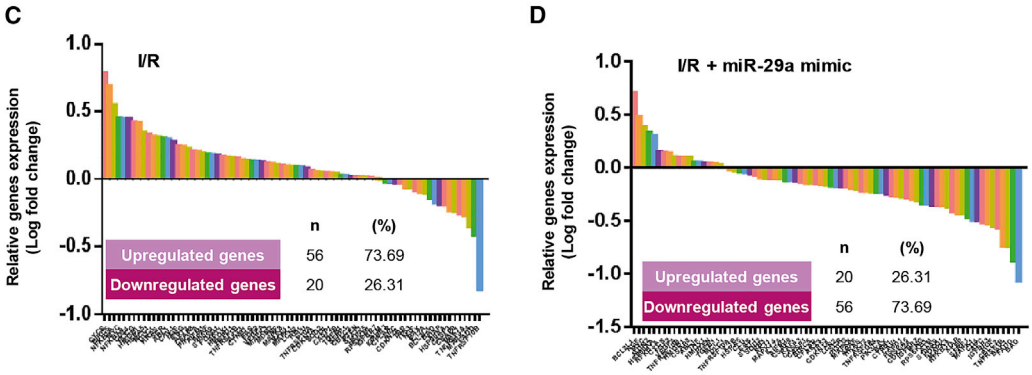
To summarize, this study demonstrates that Ucn-2 provides long-lasting cardioprotective effects involving miRNAs regulation, which target apoptosis and fibrosis. Mimicking changes of the expression of miRNAs caused by Ucn-2, combined with functional studies, this allows us to efficiently identify a new role for miR-29a in myocardial I/R, which presumably leads to a balanced regulation of anti- and pro-apoptotic pathways.

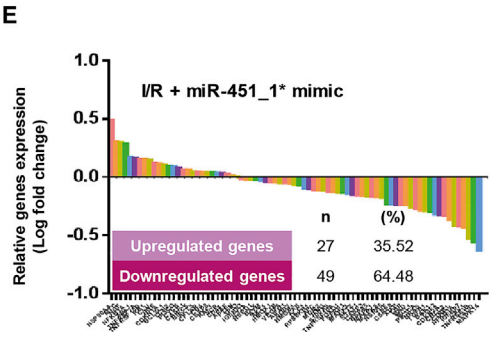
standard error of the mean (n = 8–10). (C–H) Bar graphs show the expression of miR-29a I, miR-103 (D), miR-133 (E), miR-339-5p (F), miR-423_1 (G) and miR-451_1* (H) examined in the risk zone of the infarcted heart of sham, I/R and I/R + Ucn-2, 24 h and 1 week after surgery. Relative expression levels were calculated using the $2^{-\Delta\Delta Ct}$ method after normalization to the expression of the endogenous control miRTC1. Values are relative expression of Log fold change of means ± standard error of the mean (n = 4–6). *p < 0.05; **p < 0.01; ***p < 0.001; ****p < 0.0001.



B

	Targeted Apoptosis Genes	Targeted Fibrosis Genes
miR-29a	16	14
miR-103	5	4
miR-133	15	6
miR-339-5p	3	3
miR-423_1	1	-
miR-451_1*	17	18





(legend on next page)

MATERIALS AND METHODS

This study was performed in accordance with the recommendations of the Royal Decree 53/2013 in agreement with the Directive 2010/63/EU of the European Parliament and approved by the local Ethics Committee on Human and animal Research of A Coruña and University Hospital of Virgen del Rocio of Seville.

Human blood samples and myocardial biopsies from patients with HF

Human serum was obtained from blood samples from patients who suffered a first STEMI by centrifugation at 1500 g for 15 min, as detailed in previously.[18] The inclusion criteria were patients less than 75 years old, diagnosed with AMI, presenting symptoms 2 to 6 h prior to angioplasty and exhibiting epicardial Thrombolysis in Myocardial Infarction (TIMI) flow grade of 0 in the initial angiogram. Patients with a previous history of ischemic heart disease, a glomerular filtration rate less than 30 mL/min, TIMI flow grade of greater than 1 at the time of angiography were excluded. Patients received standard pharmacological therapy as per current clinical guidelines.

Myocardial biopsies were obtained from the atrium of five males and two females with a median age of 62 years, and an LVEF of 52.8 ± 2.1%, before surgery. Left ventricle biopsies of ischemic patients with HF were obtained from four males and three females, with a median age of 58.6 years and an LVEF of 31.7 ± 6.4%. We also used one ventricle biopsy from a healthy donor. These samples were obtained from patients during surgery for cardiac transplantation at the University Hospital of Virgen del Rocio in Seville and in A Coruña Hospital. A signed informed written consent was provided from the families of all donors.

Rat model of myocardial I/R

The I/R rat model was performed using male Wistar rats weighing 250 ± 50 g as previously described.[10] Briefly, rats were anesthetized with intraperitoneal (i.p.) injection of 50 mg/kg ketamine plus 8 mg/kg xylazine and were maintained with a mixture of 2% O_2/sevoflurane during the whole procedure. A left thoracotomy was performed in the intercostal space followed by a pericardiotomy. To induce the stenosis a 6/0 Prolene (Ethicon, NJ) nylon suture was placed around the left anterior descendant coronary artery, reducing the vascular light using a small piece of PE-10 tube that was placed in between for a convenient release upon reperfusion. Analgesia was provided for 3 days after surgery.

In vivo experimental groups

As shown in Figure S1A, the experimental groups in the rat model were divided into a sham group, including rats undergoing the same surgical procedure without coronary ligation; an I/R group, where ischemia was produced by ligation of the left coronary artery during 40 min, afterward 0.9% NaCl solution was added through tail veins 5 min before reperfusion; and an I/R + Ucn-2 group, which is the same as I/R group, but an intravenous dose of Ucn-2 (150 μg/kg) was administered 5 min before reperfusion. Experiments were performed specifically in the risk zone of the infarcted heart, which sits adjacent to the areas of the artery ligature.[10,46] Three end points (24 h, 1 week, and 6 weeks) were used, depending on the experiment.

ARVMs primary culture

The hearts were removed and mounted on a Langendorff perfusion apparatus. ARVMs were isolated using collagenase type II (251 IU/mL) (Worthington Biochemical Corporation, Lakewood, NJ) as described previously.[12] Isolated cells were filtered, centrifuged, and suspended in Tyrode solution containing 130 mM NaCl, 1 mM $CaCl_2$, 0.5 mM $MgCl_2$, 5.4 mM KCl, 22 mM glucose, 25 mM HEPES, 0.4 mM NaH_2PO_4, and 5 mM $NaHCO_3$) (pH 7.4). ARVM were plated in a control solution containing 1.8 mM CaCl2 at 37°C and were later subjected to a protocol of I/R as summarized in Figure S1B, using a simulated ischemic solution of 142 mM NaCl, 3.6 mM KCl, 1.2 mM $MgCl_2$, 1.8 mM $CaCl_2$, 5 mM $NaHCO_3$, 20 mM HEPES, 20 mM Lactate-Na, and 20 mM sucrose (pH 6.22), as described previously.[13,14] Cells were placed during 30 min in an incubator at 1% O_2 and 5% CO_2. Afterward, cells were reoxygenated in control solution and maintained in at 21% O_2 and 5% CO_2 for 18–24 h. We added 30 nM Ucn-2 before reperfusion. All experiments were performed on Ca^{2+}-tolerant rod-shaped myocytes.

Neonatal rat ventricle myocytes primary culture

NRVMs were isolated from the heart of 1- to 3-day-old Wistar rats. The primary ventricular cardiac myocytes were cultured in DMEM/medium 199 (4:1) supplemented with 10% horse serum, 15% fetal bovine serum, 1% glutamine, 100 U/mL penicillin, and 100 μg/mL streptomycin for 24 h; later, the medium was replaced.

For miRNAs experiments, NRVMs were transfected at 70% of confluence, 48 h after isolation, according to the manufacturer's instructions, using Lipofectamine RNAiMAX Transfection Reagent (Thermo Fisher Scientific, Waltham, MA) with 10 μM of mimics Rno -miR 29a (5′-UAGCACCAUCUGAAAUCGGUUA-3′), Rno -miR 451 (5′AAACCGUUACCAUUACUGAGUU-3′) or negative-control (Ambion, Thermo Fisher ScientificA). Twenty-four hours later, cells were exposed to the protocol of I/R as illustrated in the Figure S1B.

For the pharmacological study, NRVM were incubated with inhibitors 10 min before their exposition to I/R ± Ucn-2 (Figure S1C).

Figure 5. miR-29a and miR-451_1* are predicted to target apoptosis-related genes

(A) PANTHER analysis showing the predicted pathways go be targeted by miR-29a, miR-103, miR-133, miR-339-5p, miR-423_1, and miR-451_1*. The pink and gray slice in the pie chart highlight predicted genes related to apoptosis and fibrosis. (B) Number of predicted target genes for each miRNA. (C–E) Graphs show of the expression of 76 dysregulated genes examined using samples (n = 4) from NRVM exposed to I/R (C), and from NRVM transfected with mimics of miR-29a (D) and miR-451_1* (E) in I/R. Inserts show numbers and percentage of upregulated and downregulated genes in each condition.

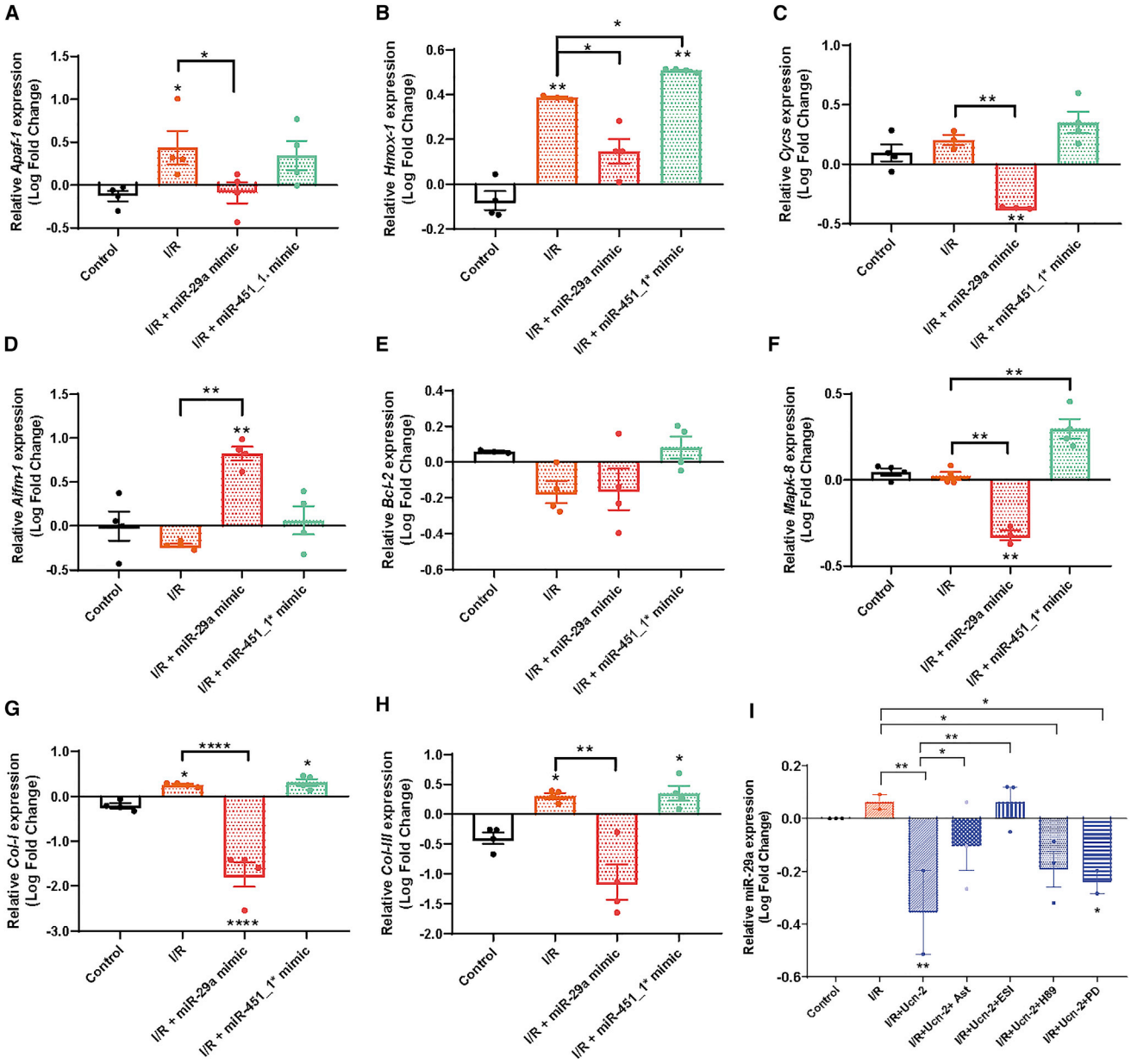


Figure 6. miR-29a regulates apoptotic and fibrotic genes under I/R, and signaling pathway of miR-29a regulation by Ucn-2

(A–F) Bar graphs showing the expression of *Apaf-1*, *Aifm-1*, *Bcl-2*, *Cycs*, *Hmox-1*, and *Mapk-8*, in control, in non-transfected NVRM under I/R (orange), and in NRVM transfected with miR-29a (red) and 451_1* (green). (G and H) Bar graphs showing the expression of *Col- I* and *Col-III* in similar conditions as in above. (I) Bar graph shows the expression of miR-29a examined in untreated NRVM "Control," in NRVM under "I/R," in NRVM treated with Ucn-2 (10 nM) before reperfusion "I/R + Ucn-2," and in NRVM pretreated with Astressin (1 μM) to inhibit CRF-R2 "I/R + Ucn-2+Ast," H89 (1 μM) to inhibit PKA "I/R + Ucn-2+H89," ESI-05 (10 μM) to block Epac2 "I/R + Ucn-2+ESI," and PD 098059 (5 μM) to inhibit ERK1/2 "I/R + Ucn-2+PD". Ucn-2 was added before reperfusion. Relative expression levels were calculated using the $2^{-\Delta\Delta Ct}$ method after normalization with the expression of the endogenous control β-actin for genes and miRTC1 for miR-29a. Values are expressed as relative expression of Log fold change of means ± standard error of the mean (n = triplicate of 3–4 cell culture). *p < 0.05; **p < 0.01; ****p < 0.0001.

Echocardiography and cardiovascular magnetic resonance

Transthoracic echocardiographic and the cardiac magnetic resonance analysis were performed as described previously.[10] The cardiac function was assessed 1 week after surgery in light anesthetized rats with 2% sevoflurane by Vevo 2100 ultrasound system with a transducer MS250 using a frequency range of 13–24 MHz (VisualSonics, Toronto, Ontario, Canada). M-Mode images of the left ventricle at the level of the papillary muscles were obtained, and functional hemodynamic

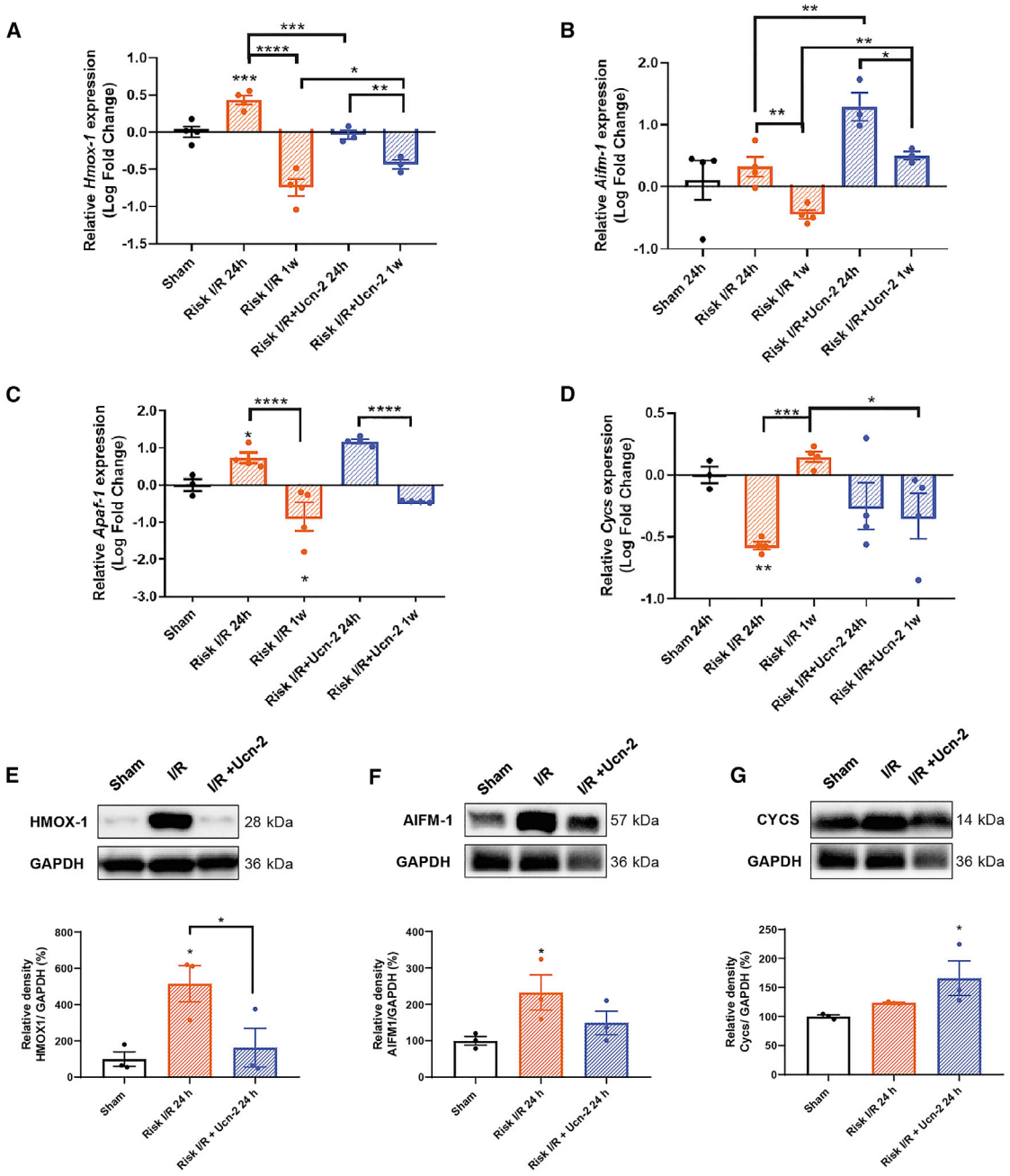


Figure 7. Expression of apoptotic genes and protein I/R rat model

(A–D) Bar graphs showing the relative expressions of *Hmox-1*, *Aifm-1*, *Apaf-1*, and *Cycs* calculated using the $2^{-\Delta\Delta Ct}$ method after normalization with the expression of the endogenous control β-actin. (E–G) Representative immunoblots and summary data of protein expression of HMOX-1, AIFM-1, and CYCS assessed by western blots and normalized to their corresponding GAPDH expression. GAPDH blots in 7F and 7G are the same. Samples were from sham, I/R, and I/R + Ucn-2 rats, and were processed 24 h and 1 week after surgery. Values are from n = 3–4. *p < 0.05; **p < 0.01; ***p < 0.001.

parameters were recorded as the LVEF, LVFS, left ventricle end-diastolic diameter, LVEdV, and LVEsV.

The cardiac magnetic resonance study was performed with the imaging system ICON 1T (Bruker, Rheinstetten, Germany) using a rat whole body coil. To quantify the ischemic area, images were collected with gradient echo T1 sequences and synchronized with the electrocardiogram (repetition time: 100 ms; echo time: 2.5 ms; resolution: 0.234 × 0.234 mm; slice thickness: 1.250 mm; angle of rotation: 75° or 90°; two cuts with the same geometry as the previous film

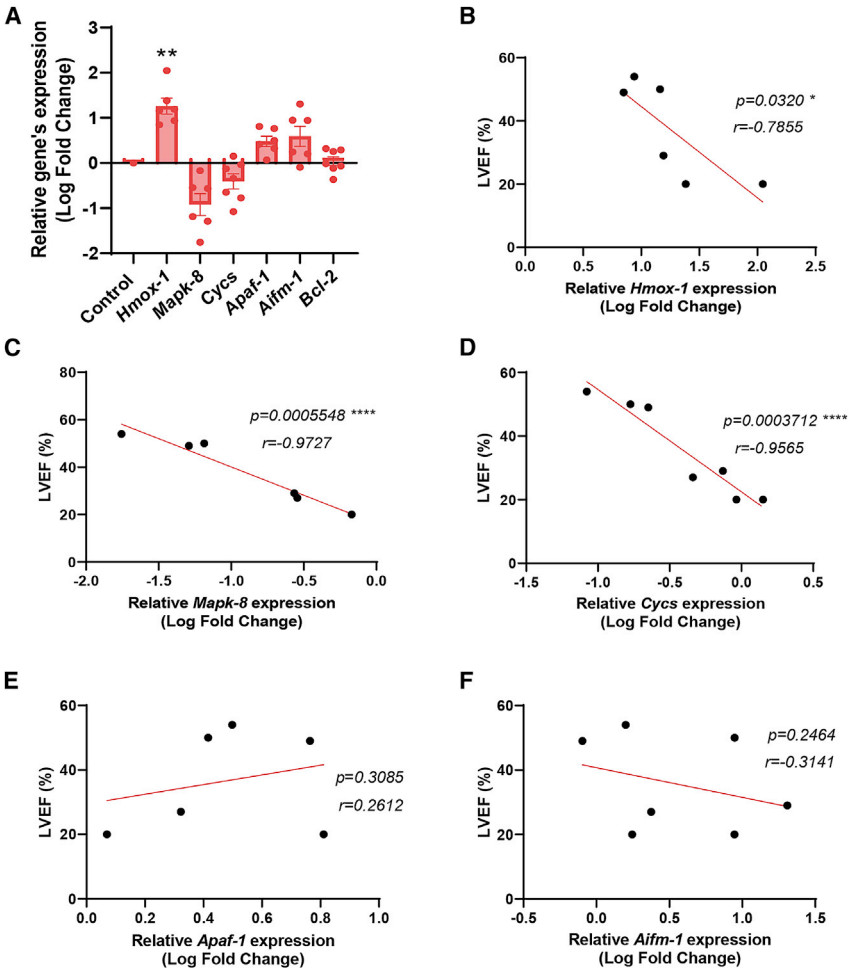


Figure 8. Expression of apoptotic genes in left ventricles of ischemic patients with HF

(A) Bar graph showing the expression of *Hmox-1*, *Mapk-8*, *Cycs*, *Apaf-1*, and *Aifm-1*, in ventricle biopsies from ischemic patients with HF, as compared to a healthy ventricle. (B–F) Graphs showing linear regression analysis using the percentage of the LVEF vs the expression of *Hmox-1*, *Mapk-8*, *Cycs*, *Apaf-1*, and *Aifm-1*. Relative expression levels were calculated using the $2^{-\Delta\Delta Ct}$ method after normalization with the expression of the endogenous control β-actin. Values are expressed as relative expression of log fold change of means ± standard error of the mean (n = 7). *p < 0.05; **p < 0.01; ****p < 0.0001.

sequences, 15 min after the introduction of a gadolinium-based contrast to highlight fibrotic areas. The acquisition of images and their analysis were performed in a blind manner.

Masson's trichrome staining

Hearts from the three experimental groups were fixed with formalin and embedded in paraffin. Hearts were cut into 6-μm sections and Masson's trichrome protocol was performed to determine fibrosis stained in blue. Tissue without fibrosis was stained in red.

TUNEL assay and cleaved caspase 3 immunofluorescence

Hearts of rats were dissected, washed in cold PBS for blood clearance, and fixed with 4% paraformaldehyde. Sections were immersed in optimal cutting temperature and frozen to −80°C and later cut into 6-μM slices. For the TUNEL assay, heart sections were stained using the in-situ Cell Death Detection Kit, with fluorescein (Roche, Basel, Switzerland) following the instruction of the manufacturer. TUNEL-positive nuclei fluoresced bright green at 480–500 nm. Images were taken by widefield Thunder microscope Leica (Leica, Wetzlar, Germany) with computational clearance at 10×.

For caspase 3 immunofluorescence, heart sections were incubated overnight with primary anti-cleaved caspase 3 antibody (Cell Signaling, Danvers, MA). After washing, sections were incubated with a secondary antibody Alexa Fluor 594 (Thermo Fisher Scientific). Wheat germ agglutinin conjugated with Alexa Fluor 488 was used to stain cell membrane, while DAPI was used to stain nuclei. Five snapshots per condition were acquired using a fluorescence microscope Olympus BX61 (Tokyo, Japan) with a 40× objective, and images were analyzed to count the different proportion of red stained cells with ImageJ 1.45 software (Wayne Rasband, National Institute of Health, Bethesda, MD).

Annexin V-fluorescein isothiocyanate staining

Annexin V-fluorescein isothiocyanate (FITC) staining was used to detect apoptosis in adult rat cardiac myocytes seeded in 6-channel μ-slides VI 0.4 (Ibidi, Gräfelfing, Germany), incubated with 100 μL of the binding buffer supplied with the kit (Trevigen, Minneapolis, MN), and 1 μL of annexin-FITC reagent, during 35 min at 25°C. Images were taken with confocal microscope Leica TCS SP2 (Leica). Five snapshots per condition were acquired using an HCX PI Apo CS dry 20× objective with 2× zoom in z-stack intervals, and the maximum projection was recorded and analyzed with ImageJ software ImageJ 1.45 software (Wayne Rasband, National Institute of Health), to count the proportion of labeled cells.

All assays were performed per triplicate, and counts were independently conducted by two people in a blind manner.

ELISA

Serum of rats from the three experimental groups were purified using separation columns. The level of Ucn-2 was determined by immunofluorescence assay (Phoenix Pharmaceuticals, Burlingame, CA) following manufacturer instructions. The level of LDH was detected by LDH-Glo Cytotoxicity Assay (Promega, Madison, WI).

RNA extraction and quantitative real-time PCR analysis

An miRNeasy Serum/Plasma kit (Qiagen, Hilden, Germany) was used to extract small RNAs from patient's serum following the manufacturer instructions. Taqman array miRNAs cards pool A (Applied Biosystem, Foster City, CA) was also used to determine changes in the expression of miRNA using Viia7 Real-Time PCR system (Applied Biosystems). The plate design includes mammalian U6, RNU44, and RNU46 as an endogenous control.

For tissue samples, miRNeasy kit (Qiagen) was used to extract total RNA or miRNAs following the manufacturer's instructions. Samples were quantified using Nanodrop (Thermo Fisher Scientific) for RNA and by Qubit (Thermo Fisher Scientific) for miRNAs. Reverse transcription reactions were performed using miScript II RT Kit (Qiagen) (500 ng), in accordance with the manufacturer's protocols. Prior to quantitative real-time PCR reactions, cDNA was diluted 1 in 5 for PCR assays.

PCR assays of miRNAs were performed using 10× universal primer (miScript SYBR Green PCR Kit, Qiagen), Sybr Green reactive (iTaq Universal SYBR Green Supermix, Bio-Rad), and specific oligos of each miRNA: miR-103, miR-125a, miR-133, miR-139, miR-29a, miR-320, miR-324-3p, miR-324-5p, miR-339-5p, miR-423_1, miR-451_1*, and miR-499_1 (Qiagen) according to the manufacturer instructions, using a ViiA 7 Real-Time PCR System (Applied Biosystems). The average expression levels of miRNAs in cells were normalized to miRTC1.

Reactions for genes PCR assays were performed in a 10-μL reaction mixture volume with 100 nM forward primer and 100 nM reverse primer for mRNA. Primer sequences are described in Table S2. The average expression levels of genes were normalized to β-actin.

ViiA 7 Software version 1.2 (Life Technologies, Carlsbad, CA) was used to calculate the quantification cycle (Ct) value, which is defined as the number of cycles at which the fluorescence signal is significantly above the threshold; expression of each mRNA and miRNA was defined from the threshold cycle (Ct), and relative expression levels were calculated using the $2^{-\Delta\Delta Ct}$ method after normalization with the internal control, miRTC1 and β-actin for miRNA and mRNA, respectively. Data are expressed as relative expression of log fold change of means ± standard error of the mean of at least four replicates of each experiment.

PrimePCR assay

We used PrimePCR (Bio-Rad) predesigned assay (Apoptosis and Survival Tier 1 H96), containing primers of validated genes specifically for apoptosis and survival pathway, as indicated in Table S1 and Figure 2. A mix of four samples was added and the reaction was performed according to the manufacturer's instructions, on a Viia7 Real-Time PCR system (Applied Biosystems). The average expression levels of genes were normalized to the expression of housekeeping gene HPRT1.

In silico analysis of targeted genes by miRNAs

The analysis of targeted genes predicted to be regulated by miRNAs was done using different bioinformatics resources: miRBD (miRDB v7.2, http://mirdb.org, Washington University St. Louis, MO), TargetScan (Release 7.1, www.targetscan.org, Cambridge, MA) databases, and Exiqon tool application (http://www.exiqon.com/microrna-target-prediction). To identify miRNA target gene pathways, we also used the online platform Gene Ontology browser PANTHER (Protein Analysis THrough Evolutionary Relationships) v14.1 (http://pantherdb.org/genelistanalysis.do, University of Southern California, Los Angeles, CA).

Western blotting

Protein extraction was carried out using NP40 Cell Lysis Buffer (Thermo Fisher Scientific) and quantified by Bradford method. Rat heart tissue was pre-lysed using TissueLyser II (Qiagen) before protein lysis buffer addition. Protein samples were subjected to SDS-PAGE (10% acrylamide) and electrotransferred onto PVDF membranes. After blocking with 5% non-fat dry milk dissolved in Tris-buffered saline containing 0.1% Tween 20 (TTBS) for 1 h at 37°C, membranes were probed overnight at 4°C with anti-CRF-R2 (Novus, Centennial, CO), anti-tubulin (Merck-Sigma-Aldrich), anti-HMOX1 (Cell Signaling), anti-AIFM1 (Cell Signaling), and anti-GAPDH (Sigma-Aldrich), in TTBS with 1% BSA. After washing, membranes were incubated for 45 min at room temperature with a horseradish peroxidase conjugated with anti-IgG (Cell Signaling). Detection was performed in the ImageQuant LAS 4000 mini (GE Healthcare, Chicago, IL). Images were analyzed with ImageJ software (NIH).

Statistical analysis

Analyzes were performed with GraphPad (GraphPad Software, Inc., La Jolla, CA), using Shapiro-Wilk as normality test. For normally distributed variables we used the ordinary one-way ANOVA, and we performed the multiples comparisons using *t* test without correction (Fisher's least significant differences test). We also used the non-parametric test Kruskal-Wallis with multiple comparisons corrected by Dunn's Test for non-normally distributed variables. Values were subjected to log-transformation to represent numerical features in the dataset to have a mean of 0 and a variance of 1 and to express data as relative gene/miR expression (log fold change). The outliers were removed based on results of QuickCalcs, an online tool of Graphpad. Results are presented as the mean ± standard error of the mean.

SUPPLEMENTAL INFORMATION

Supplemental information can be found online at https://doi.org/10.1016/j.omtn.2022.01.003.

ACKNOWLEDGMENTS

The authors thank Eva Sanchez de Rojas de Pedro for her technical help. The graphical abstract was created with Biorender.com (http://biorender.io).

This study was co-financed by FEDER Funds [US-1381135], Agencia Estatal de Investigación [PID2019-104084GB-C22/AEI/10.13039/

501100011033]; the Institute of Carlos III [PI18/01197; Red TerCel-Grant RD16/0011/0034]; the Andalusia Government [grant number: PI-0193-2018]; and by Agence National de la Recherche [ANR-19-14-0031-01].

AUTHOR CONTRIBUTIONS

Conceptualization, A.H., and T.S.; funding acquisition, A.H., A.O., E.C.-S., and T.S.; investigation, I.M.-G., E.C.-S., I.G.-O, E.G.-C, A.O., and T.S.; methodology, I.M.-G., E.C.-S., I.G.-O, M.M.B., N.D., A.G., M.F.-V., A.H., and T.S.; project administration, A.O., and T.S.; writing—original draft, I.M.-G. and T.S.; and writing—review and editing, N.D., M.C.-L, M.F.-V., A.G., D.-R.A., A.O., A.H., and T.S.

DECLARATION OF INTERESTS

The authors declare that the research was conducted in the absence of any commercial or financial relationships that could be interpreted as a potential conflict of interest.

REFERENCES

1. Bahit, M.C., Kochar, A., and Granger, C.B. (2018). Post-myocardial infarction heart failure. JACC Heart Fail. *6*, 179–186.
2. Abbate, A., and Narula, J. (2012). Role of apoptosis in adverse ventricular remodeling. Heart Fail. Clin. *8*, 79–86.
3. Feuerstein, G.Z. (2001). Apoptosis - new opportunities for novel therapeutics for heart diseases. Cardiovasc. Drugs Ther. *15*, 547–551.
4. Yellon, D.M., and Hausenloy, D.J. (2007). Myocardial reperfusion injury. N. Engl. J. Med. *357*, 1121–1135.
5. Eltzschig, H.K., and Eckle, T. (2011). Ischemia and reperfusion-from mechanism to translation. Nat. Med. *17*, 1391–1401.
6. González-Montero, J., Brito, R., Gajardo, A.I., and Rodrigo, R. (2018). Myocardial reperfusion injury and oxidative stress: therapeutic opportunities. World J. Cardiol. *10*, 74–86.
7. Monteiro-Pinto, C., Adão, R., Leite-Moreira, A.F., and Brás-Silva, C. (2019). Cardiovascular effects of urocortin-2: pathophysiological mechanisms and therapeutic potential. Cardiovasc. Drugs Ther. *33*, 599–613.
8. Van Pett, K., Viau, V., Bittencourt, J.C., Chan, R.K.W., Li, H.Y., Arias, C., Prins, G.S., Perrin, M., Vale, W., and Sawchenko, P.E. (2000). Distribution of mRNAs encoding CRF receptors in brain and pituitary of rat and mouse. J. Comp. Neurol. *428*, 191–212.
9. Smani, T., Calderon, E., Rodriguez-Moyano, M., Dominguez-Rodriguez, A., Diaz, I., and Ordóñez, A. (2011). Urocortin-2 induces vasorelaxation of coronary arteries isolated from patients with heart failure. Clin. Exp. Pharmacol. Physiol. *38*, 71–76.
10. Domínguez-Rodríguez, A., Mayoral-Gonzalez, I., Avila-Medina, J., de Rojas-de Pedro, E.S., Calderón-Sánchez, E., Díaz, I., Hmadcha, A., Castellano, A., Rosado, J.A., Benitah, J.-P., et al. (2018). Urocortin-2 prevents dysregulation of Ca2+ homeostasis and improves early cardiac remodeling after ischemia and reperfusion. Front. Physiol. *9*, 813.
11. Calderón-Sanchez, E., Delgado, C., Ruiz-Hurtado, G., Domínguez-Rodríguez, A., Cachofeiro, V., Rodríguez-Moyano, M., Gomez, A.M., Ordóñez, A., and Smani, T. (2009). Urocortin induces positive inotropic effect in rat heart. Cardiovasc. Res. *83*, 717–725.
12. Calderón-Sánchez, E.M., Ruiz-Hurtado, G., Smani, T., Delgado, C., Benitah, J.P., Gómez, A.M., and Ordóñez, A. (2011). Cardioprotective action of urocortin in postconditioning involves recovery of intracellular calcium handling. Cell Calcium *50*, 84–90.
13. Calderón-Sánchez, E., Díaz, I., Ordóñez, A., and Smani, T. (2016). Urocortin-1 mediated cardioprotection involves XIAP and CD40-ligand recovery: role of EPAC2 and ERK1/2. PLoS One *11*, e0147375.
14. Díaz, I., Calderón-Sánchez, E., Toro, R.D., Ávila-Médina, J., de Rojas-de Pedro, E.S., Domínguez-Rodríguez, A., Rosado, J.A., Hmadcha, A., Ordóñez, A., and Smani, T. (2017). miR-125a, miR-139 and miR-324 contribute to Urocortin protection against myocardial ischemia-reperfusion injury. Sci. Rep. *7*, 8898.
15. Smani, T., Mayoral-Gonzalez, I., Galeano-Otero, I., Gallardo-Castillo, I., Rosado, J.A., Ordoñez, A., and Hmadcha, A. (2020). Non-coding RNAs and ischemic cardiovascular diseases. Adv. Exp. Med. Biol. *1229*, 259–271.
16. Nabeebaccus, A., Zheng, S., and Shah, A.M. (2016). Heart failure-potential new targets for therapy. Br. Med. Bull. *119*, 99–110.
17. Lucas, T., Bonauer, A., and Dimmeler, S. (2018). RNA therapeutics in cardiovascular disease. Circ. Res. *123*, 205–220.
18. Galeano-Otero, I., Del Toro, R., Guisado, A., Díaz, I., Mayoral-González, I., Guerrero-Márquez, F., Gutiérrez-Carretero, E., Casquero-Domínguez, S., Díaz-de la Llera, L., Barón-Esquivias, G., et al. (2020). Circulating miR-320a as a predictive biomarker for left ventricular remodelling in STEMI patients undergoing primary percutaneous coronary intervention. J. Clin. Med. *9*, 1051.
19. Fasanaro, P., D'Alessandra, Y., Di Stefano, V., Melchionna, R., Romani, S., Pompilio, G., Capogrossi, M.C., and Martelli, F. (2008). MicroRNA-210 modulates endothelial cell response to hypoxia and inhibits the receptor tyrosine kinase ligand Ephrin-A3. J. Biol. Chem. *283*, 15878–15883.
20. Yano, Y., Ozono, R., Oishi, Y., Kambe, M., Yoshizumi, M., Ishida, T., Omura, S., Oshima, T., and Igarashi, K. (2006). Genetic ablation of the transcription repressor Bach1 leads to myocardial protection against ischemia/reperfusion in mice. Genes Cells *11*, 791–803.
21. Basaiyye, S.S., Naoghare, P.K., Kanojiya, S., Bafana, A., Arrigo, P., Krishnamurthi, K., and Sivanesan, S. (2018). Molecular mechanism of apoptosis induction in Jurkat E6-1 cells by Tribulus terrestris alkaloids extract. J. Tradit. Complement. Med. *8*, 410–419.
22. Gao, Z., Gao, Q., and Lv, X. (2020). MicroRNA-668-3p protects against oxygen-glucose deprivation in a rat H9c2 cardiomyocyte model of ischemia-reperfusion injury by targeting the stromal cell-derived factor-1 (SDF-1)/CXCR4 signaling pathway. Med. Sci. Monit. *26*, e919601.
23. Rivier, J., Gulyas, J., Kirby, D., Low, W., Perrin, M.H., Kunitake, K., DiGruccio, M., Vaughan, J., Reubi, J.C., Waser, B., et al. (2002). Potent and long-acting corticotropin releasing factor (CRF) receptor 2 selective peptide competitive antagonists. J. Med. Chem. *45*, 4737–4747.
24. Rehmann, H. (2013). Epac-inhibitors: facts and artefacts. Sci. Rep. *3*, 1–6.
25. Keiper, M., Stope, M.B., Szatkowski, D., Böhm, A., Tysack, K., Vom Dorp, F., Saur, O., Oude Weernink, P.A., Evellin, S., Jakobs, K.H., et al. (2004). Epac- and Ca2+-controlled activation of Ras and extracellular signal-regulated kinases by Gs-coupled receptors. J. Biol. Chem. *279*, 46497–46508.
26. Smani, T., Calderón-Sanchez, E., Gómez-Hurtado, N., Fernández-Velasco, M., Cachofeiro, V., Lahera, V., Ordoñez, A., and Delgado, C. (2010). Mechanisms underlying the activation of L-type calcium channels by urocortin in rat ventricular myocytes. Cardiovasc. Res. *87*, 459–466.
27. Heusch, G. (2020). Myocardial ischaemia–reperfusion injury and cardioprotection in perspective. Nat. Rev. Cardiol. *17*, 773–789.
28. Wright, S.P., Doughty, R.N., Frampton, C.M., Gamble, G.D., Yandle, T.G., and Richards, A.M. (2009). Plasma urocortin 1 in human heart failure. Circ. Heart Fail. *2*, 465–471.
29. Tang, W.H.W., Shrestha, K., Martin, M.G., Borowski, A.G., Jasper, S., Yandle, T.G., Richards, A.M., Klein, A.L., and Troughton, R.W. (2010). Clinical significance of endogenous vasoactive neurohormones in chronic systolic heart failure. J. Card. Fail. *16*, 635–640.
30. Giamouridis, D., Gao, M.H., Lai, N.C., Guo, T., Miyanohara, A., Blankesteijn, W.M., Biessen, E.A.L., and Hammond, H.K. (2020). Urocortin 2 gene transfer improves heart function in aged mice. Mol. Ther. *28*, 180–188.
31. Giamouridis, D., Gao, M.H., Lai, N.C., Tan, Z., Kim, Y.C., Guo, T., Miyanohara, A., Blankesteijn, W.M., Biessen, E., and Hammond, H.K. (2018). Effects of urocortin 2 versus urocortin 3 gene transfer on left ventricular function and glucose disposal. JACC Basic Transl. Sci. *3*, 249–264.

32. Zhou, Y., Chen, Q., Lew, K.S., Richards, A.M., and Wang, P. (2016). Discovery of potential therapeutic miRNA targets in cardiac ischemia-reperfusion injury. J. Cardiovasc. Pharmacol. Ther. *21*, 296–309.

33. Xiao, L., He, H., Ma, L., Da, M., Cheng, S., Duan, Y., Wang, Q., Wu, H., Song, X., Duan, W., et al. (2017). Effects of miR-29a and miR-101a expression on myocardial interstitial collagen generation after aerobic exercise in myocardial-infarcted rats. Arch. Med. Res. *48*, 27–34.

34. Qin, R.H., Tao, H., Ni, S.H., Shi, P., Dai, C., and Shi, K.H. (2018). microRNA-29a inhibits cardiac fibrosis in Sprague-Dawley rats by downregulating the expression of DNMT3A. Anatol. J. Cardiol. *20*, 198–205.

35. Jing, X., Yang, J., Jiang, L., Chen, J., and Wang, H. (2018). MicroRNA-29b regulates the mitochondria-dependent apoptotic pathway by targeting Bax in doxorubicin cardiotoxicity. Cell. Physiol. Biochem. *48*, 692–704.

36. Shakeri, R., Kheirollahi, A., and Davoodi, J. (2017). Apaf-1: regulation and function in cell death. Biochimie *135*, 111–125.

37. Wang, Y., Zhang, Q., Zhong, L., Lin, M., Luo, X., Liu, S., Xu, P., Liu, X., and Zhu, Y.Z. (2017). Apoptotic protease activating factor-1 inhibitor mitigates myocardial ischemia injury via disturbing procaspase-9 recruitment by apaf-1. Oxid. Med. Cell. Longev. *2017*, 9747296.

38. Sanchis, D., Mayorga, M., Ballester, M., and Comella, J.X. (2003). Lack of Apaf-1 expression confers resistance to cytochrome c-driven apoptosis in cardiomyocytes. Cell Death Differ. *10*, 977–986.

39. Bilbija, D., Gravning, J.A., Haugen, F., Attramadal, H., and Valen, G. (2012). Protecting the heart through delivering DNA encoding for heme oxygenase-1 into skeletal muscle. Life Sci. *91*, 828–836.

40. Preda, M.B., Rønningen, T., Burlacu, A., Simionescu, M., Moskaug, J.Ø., and Valen, G. (2014). Remote transplantation of mesenchymal stem cells protects the heart against ischemia-reperfusion injury. Stem Cells *32*, 2123–2134.

41. Czibik, G., Gravning, J., Martinov, V., Ishaq, B., Knudsen, E., Attramadal, H., and Valen, G. (2011). Gene therapy with hypoxia-inducible factor 1 alpha in skeletal muscle is cardioprotective in vivo. Life Sci. *88*, 543–550.

42. Depre, C., and Taegtmeyer, H. (2000). Metabolic aspects of programmed cell survival and cell death in the heart. Cardiovasc. Res. *45*, 538–548.

43. Zhang, S., Yin, Z., Dai, F., Wang, H., Zhou, M., Yang, M., Zhang, S., Fu, Z., Mei, Y., Zang, M., et al. (2019). miR-29a attenuates cardiac hypertrophy through inhibition of PPARδ expression. J. Cell. Physiol. *234*, 13252–13262.

44. Caravia, X.M., Fanjul, V., Oliver, E., Roiz-Valle, D., Morán-Álvarez, A., Desdín-Micó, G., Mittelbrunn, M., Cabo, R., Vega, J.A., Rodríguez, F., et al. (2018). The microRNA-29/PGC1α regulatory axis is critical for metabolic control of cardiac function. PLoS Biol. *16*, e2006247.

45. Tomczyk, M., Kraszewska, I., Dulak, J., and Jazwa-Kusior, A. (2019). Modulation of the monocyte/macrophage system in heart failure by targeting heme oxygenase-1. Vascul. Pharmacol. *112*, 79–90.

46. van Rooij, E., Sutherland, L.B., Thatcher, J.E., DiMaio, J.M., Naseem, R.H., Marshall, W.S., Hill, J.A., and Olson, E.N. (2008). Dysregulation of microRNAs after myocardial infarction reveals a role of miR-29 in cardiac fibrosis. Proc. Natl. Acad. Sci. U S A *105*, 13027–13032.